

# MARBLENET: DEEP 1D TIME-CHANNEL SEPARABLE CONVOLUTIONAL NEURAL NETWORK FOR VOICE ACTIVITY DETECTION

Fei Jia , Somshubra Majumdar , Boris Ginsburg

NVIDIA, Santa Clara, USA

## ABSTRACT

We present *MarbleNet*, an end-to-end neural network for Voice Activity Detection (VAD). *MarbleNet* is a deep residual network composed from blocks of 1D time-channel separable convolution, batch-normalization, ReLU and dropout layers. When compared to a state-of-the-art VAD model, *MarbleNet* is able to achieve similar performance with roughly 1/10-th the parameter cost. We further conduct extensive ablation studies on different training methods and choices of parameters in order to study the robustness of *MarbleNet* in real-world VAD tasks.

**Index Terms**— voice activity detection, automatic speech recognition, neural networks, depth-wise separable convolution

## 1. INTRODUCTION

Voice Activity Detection (VAD), also known as *speech activity detection* or *speech detection*, is a binary classification task of inferring which segments of input audio contain speech versus which segments are background noise. It is an essential first step for a variety of downstream speech-based applications such as automatic speech recognition and speaker diarization. A typical VAD system is a frame-level classifier using acoustic features to determine whether the frame (usually an audio segment of 10ms duration) belongs to a speech or non-speech class.

Apart from statistical modeling approaches [21, 23], recent research effort has been devoted to finding efficient deep-learning-based VAD model architectures. Notable examples include Recurrent Neural Networks (RNN) [8, 6, 16], Convolutional Neural Networks (CNN) [2, 1, 11, 25], and Convolutional Long Short-Term Memory (LSTM) Deep Neural Networks (CLDNN) [27], which conduct frequency modeling with CNN and temporal modeling with LSTM. LSTM is a popular choice for sequential modeling of VAD tasks [28, 8]. It has been observed that LSTMs suffer from state saturation problems when the utterance is long. To address this issue, Chang et al. [1] proposed a stateless dilated CNN (with 400K parameters) for temporal modeling. Thomas et al. [25] found severe performance degradation when the VAD models were evaluated on unseen audio recorded from radio channels. They also demonstrated that CNNs were useful acoustic models in novel channel scenarios and able to adapt well with limited amounts of data. Hebbbar et al. [11] compared different LSTM and CNN models with more challenging movie data which contained post-production stage and atypical speech such as electronically modified speech samples. They proposed a Convolutional Neural Network-Time Distributed (CNN-TD) model (with 740K parameters) that outperformed existing models including Bi-LSTM (with 300K parameters) and CLDNN (with 1M parameters) on the benchmark evaluation dataset *AVA-speech*. Furthermore, acoustic models using temporal CNNs have

shown great potential in automatic speech recognition [14, 17, 18] and speech command detection [19] tasks.

Built on top of previous successful applications of temporal CNNs to speech processing tasks, we introduce *MarbleNet*, a compact end-to-end neural network for VAD inspired by the QuartzNet architecture [14] and the MatchboxNet model [19]. *MarbleNet* is constructed with a stack of blocks with residual connections [9]. Each block is composed from 1D time-channel separable convolutions, batch normalization, ReLU, and dropout layers. Those 1D time-channel separable convolutions are similar to 2D depth-wise separable convolutions [3, 12]. The usage of 1D time-channel separable convolutions significantly reduces the number of parameters in the model. *MarbleNet* has a parameter count roughly 1/10-th that of regular 1D convolutional models [14], enabling more efficient model inference and storage. With increasingly widespread usage of speech-based applications across mobile and wearable devices (e.g., virtual assistant), building lightweight VAD models carries important implications for real-world applications in memory and compute constrained deployment scenarios.

Specifically, this paper makes the following contributions:

1. We propose MarbleNet: a novel end-to-end neural model for VAD based on 1D time-channel separable convolutions.
2. MarbleNet achieves state-of-the-art performance on the AVA speech dataset [2], and it has 10x fewer parameters compared to the CNN-TD model [11].
3. We perform ablation studies for model and training parameters including input features, noise augmentation, and overlapped predictions.
4. We open source the model, training and inference pipelines together with pre-trained checkpoints for easy reproduction of presented results.

## 2. MODEL ARCHITECTURE

*MarbleNet-BxRxC* is based on the QuartzNet architecture. It includes  $B$  residual blocks each with  $R$  sub-blocks. All sub-blocks within each block have the same  $C$  output channels (see Fig. 1). A basic sub-block consists of a 1D-time-channel separable convolution, 1x1 pointwise convolutions, batch norm, ReLU, and dropout. The 1D time-channel separable convolution has  $C$  filters with a kernel of the size  $K$ . All models have four additional sub-blocks: one prologue layer – ‘Conv1’ before the first block, and three epilogue sub-blocks (‘Conv2’, ‘Conv3’, and ‘Conv4’) before the final softmax layer. For example, the complete architecture for *MarbleNet-3x2x64* ( $B=3$  blocks,  $R=2$  sub-blocks per block,  $C=64$  channels) is shown in the Table 1.

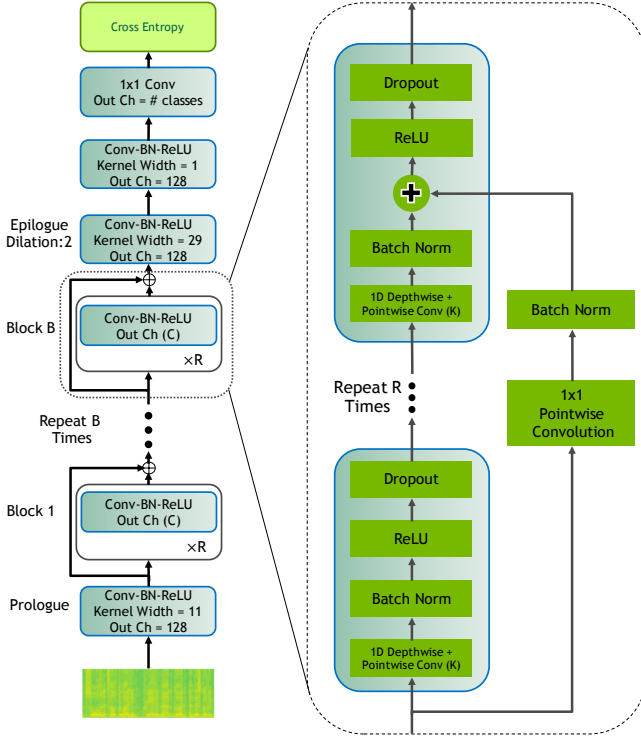


**Fig. 1.** MarbleNet  $B \times R \times C$  model:  $B$  - number of blocks,  $R$  - number of sub-blocks,  $C$  - the number of channels.

### 3. EXPERIMENTS

#### 3.1. Training Data

Generally, noise-robust VAD systems are developed using audio from clean speech datasets augmented with different types of noise [5, 11, 16]. Hebbar et al. [11] compiled the Subtitle-Aligned Movie (SAM) corpus, a dataset based on 117 hours of movie audio. However, the SAM dataset is constructed from movies, some of which are restricted from commercial usage. Therefore, we use Google Speech Commands Dataset V2 [26] as speech data. This dataset contains 105,000 utterances, each approximately 1s long, belonging to one of 35 classes of common words like “Yes” and “Go”. Around 2,700 variable-length samples of 35 background categories such as “traffic noise”, “inside, small room” from freesound.org [7] served as non-speech data. Each sample was between 0.63s to 100s. The speech commands dataset and Freesound dataset are referred to as the *SCF* dataset hereafter. We split SCF into train, validation and test sets using an 8:1:1 ratio.

Following Hebbar et al. [11], the samples were converted to segments of length 0.63s, so that the input 64 dimensional mel-filterbank features calculated from 25ms windows with a 10ms overlap would be of shape 64x64 when provided to CNN models, for fair comparison with Hebbar et al. [11]. For speech samples in the train and validation sets, we used the central segment (0.2s-0.83s) of each sample. Speech segments in the test set and non-speech segments were generated with stride length 0.15s. We re-balanced SCF speech and non-speech classes to have the same number of segments in each of the classes. In total, 160,994, 20,018 and 60,906 segments were used for training, validation and testing respectively.

**Table 1.** *MarbleNet-3x2x64* model has  $B=3$  blocks, each block has  $R=2$  time-channel separable convolutional sub-blocks with  $C=64$  channels, plus 4 additional sub-blocks: prologue - Conv1, and epilogue - Conv2, Conv3, Conv4).

Block	# Blocks	# Sub Blocks	# Output Channels	Kernel
Conv1	1	1	128	11
B1	1	2	64	13
B2	1	2	64	15
B3	1	2	64	17
Conv2	1	1	128	29, dilation=2
Conv3	1	1	128	1
Conv4	1	1	# classes	1
Soft-max				
Cross-entropy				

#### 3.2. Training Methodology

We pre-processed the audio segments with 64 MFCC features for training *MarbleNet*. Then, with a probability of 80%, the input was augmented with time shift perturbations in the range of  $T = [-5, 5]$  ms and white noise of magnitude  $[-90, -46]$  dB. Additionally, we applied SpecAugment [20] with 2 continuous time masks of size  $[0, 25]$  time steps, and 2 continuous frequency masks of size  $[0, 15]$  frequency bands. We also used SpecCutout [4] with 5 rectangular masks in the time and frequency dimensions.

All models were trained with the SGD optimizer with momentum [24], using momentum = 0.9 and weight decay = 0.001. We utilized the Warmup-Hold-Decay learning rate schedule [10] with a warm-up ratio of 5%, a hold ratio of 45%, and a polynomial (2nd order) decay for the remaining 50% of the schedule. A maximum learning rate of 0.01 and a minimum learning rate of 0.001 were used. We trained all models for 150 epochs on 2 V100 GPUs with a batch size of 128 per GPU. The model was implemented and trained with NeMo, an open-source toolkit for Conversational AI [15].<sup>1</sup>

#### 3.3. Evaluation Method

We use the CNN-TD model proposed by Hebbar et al. [11] as our baseline. In order to compare our model with CNN-TD and examine the ability of the model to generalize to samples outside of the training domain, we evaluate our models on the AVA-speech dataset [2]. AVA-speech is a public, multi-language, densely labelled dataset of YouTube videos with one non-speech class and three speech conditions: clean speech (“clean”), speech with noise (“+noise”), and speech with music (“+music”). Each instance in the AVA-speech dataset is a 15-minute movie clip. It has a natural mix of background noise conditions, as opposed to synthetic (white/pink) noise. The dataset only contains labels for video segments, and in order to evaluate models, we still need to access the corresponding videos on YouTube. We use 122 out of 160 labelled movies that are still publicly available on YouTube at the time of the experiment as our AVA-speech evaluation dataset, totaling 30 hours of playback time. For each speech condition, we calculate the true positive rate (TPR) at the frame level contrasted with non-speech as the negative class. Moreover, we combine all the frames for the 3 speech conditions into a single positive class (“All”).

We follow Hebbar et al. [11] and report the true positive rate (TPR) when the false positive rate (FPR) equals 0.315. Since the TPR for FPR=0.315 is only a single point on the receiver operat-

<sup>1</sup><https://github.com/NVIDIA/NeMo>.

**Table 2.** Model performance on the AVA-speech dataset [2]. We report the true positive rate (TPR) when the false positive rate (FPR) equals 0.315 to compare results with Hebbar et al. [11], and report AUROC for the “All” category in AVA-speech to demonstrate the overall TPR-FPR trade-off. CNN-TD follows the reported methodology in Hebbar et al. [11] and is obtained after a hyperparameter search using the SCF validation set. We generate predictions by overlapping input segments with 87.5% overlap and adopting a median smoothing filter. Each result is averaged over 5 trials (95% Confidence Interval). Since we observed a large variance in the scores for the CNN-TD model, we report the results averaged over 10 trials.

Model	# Parameters (K)	TPR for FPR = 0.315				AUROC
		Clean	+Noise	+Music	All	All
CNN-TD	738	0.911±0.063	0.795±0.056	0.797±0.048	0.827±0.055	0.821±0.055
CNN-TD + 87.5% median	738	0.935±0.057	<b>0.824±0.051</b>	0.824±0.043	0.855±0.050	0.841±0.050
<i>MarbleNet</i> -3x2x64	88	0.924±0.005	0.815±0.014	0.822±0.017	0.847±0.012	0.850±0.009
<i>MarbleNet</i> -3x2x64 + 87.5% median	<b>88</b>	<b>0.942 ± 0.008</b>	0.821±0.022	<b>0.834±0.016</b>	<b>0.858±0.016</b>	<b>0.858±0.011</b>

ing characteristic (ROC) curve, we also report the area under ROC (AUROC) representing the overall TPR-FPR trade-off.

To eliminate the potential dataset quality difference, instead of using the saved checkpoint trained on a different dataset, we re-trained and tuned the CNN-TD model on our SCF train set. We followed the exact training procedure as the authors describe in their paper. During model training, we used a batch-size of 64, and a binary cross-entropy loss function. Mel spectrogram was used as the input feature. We trained the network for 5 epochs and performed early stopping if validation loss did not decrease by  $1e-3$  for 3 consecutive epochs. The Adam [13] optimizer was used with learning rate  $1e-4$ . We note that we also experimented extensively with other training procedures, input features, and hyper-parameter choices, and eventually determined that the default setup described above produced the best performing model for the CNN-TD baseline. CNN-TD experiment results reported below are produced with the above setup.

During inference, we performed frame-level prediction by two approaches: 1) shift the window by 10ms to generate the frame and use the prediction of the window to represent the label for the frame; 2) generate predictions with overlapping input segments. Then a smoothing filter is applied to decide the label for a frame spanned by multiple segments. We examined two common smoothing filters: majority vote (median) [11] and average (mean) [16]. We also experimented with different amounts of overlap ranging from 12.5% to 87.5% to understand the effect of this parameter for frame-level performance. The results are shown in Table 4.

### 3.4. Results

Table 2 shows the evaluation results on the AVA-speech dataset. We repeated each trial 5 times for *MarbleNet*, and 10 times for CNN-TD as we observed greater variance in the performance of this model. *MarbleNet* results display a smaller confidence interval, suggesting *MarbleNet* achieves stable training over many runs.

*MarbleNet*-3x2x64 achieves similar performance as CNN-TD but has roughly 1/10th the number of parameters. This result demonstrates that even when trained on a relatively simple training dataset (SCF train set), *MarbleNet*-3x2x64 can still obtain good test performance for the more challenging AVA-speech dataset without additional fine-tuning.

### 3.5. Ablation Study

We conducted a series of ablation studies to investigate the impact of input features, inference methods, and noise augmentation on model

performance.

#### 3.5.1. MFCC vs Mel spectrogram

We first compare the two choices of potential preprocessing and feature extraction methods for audio signals: Mel spectrogram and MFCC. They are examined with a *MarbleNet*-3x2x64 model. As shown in Table 3, MFCC outperforms Mel spectrogram on AVA-speech. When FPR equals 0.315, MFCC increases TPR by 0.030 on “clean” speech and has even greater improvements of 0.078 and 0.079 on two “noisy” speech classes respectively. These results align with the fact that the compressible lower-order cepstral coefficients of MFCC represent simple aspects of the spectral envelope. Coefficients in MFCC are less correlated and contain most of the information about the overall spectral shape. In contrast, high-order coefficients in Mel spectrogram are closer to noise and of less importance. We show an example in Figure 2, and it is visually apparent that MFCC (bottom panel) produces better inference than Mel spectrogram (top panel).

**Table 3.** Model performance of *MarbleNet*-3x2x64 under the same training methodology but with two different input features, MFCC and Mel spectrogram, on AVA-speech dataset. Each result is averaged over 5 trials (95% Confidence Interval).

Feature	TPR for FPR=0.315				AUROC
	Clean	+Noise	+Music	All	All
MFCC	0.92±0.01	0.82±0.01	0.82±0.02	0.85±0.01	0.85±0.01
Mel spectrogram	0.89±0.02	0.74±0.02	0.74±0.03	0.77±0.04	0.80±0.01

#### 3.5.2. Segment length

People speak at different speeds and their pauses might be shorter than our segment length 0.63s. If we want to detect short pauses or a speaker change within a short time, a smaller segment length could help. Since our model is fully convolutional, instead of re-training on a smaller segment length, we can simply feed in smaller segments as input data for inference. Nevertheless, because AVA-speech’s ground truth labels do not account for very short pauses, using shorter input segments does not significantly affect the model’s performance.

Figure 3 shows such an example of varying input segment lengths. Shorter segment inputs indeed allow us to detect more pauses (green lines), however the ground truth labels (red lines) mark the entire latter part of the example as “speech”.

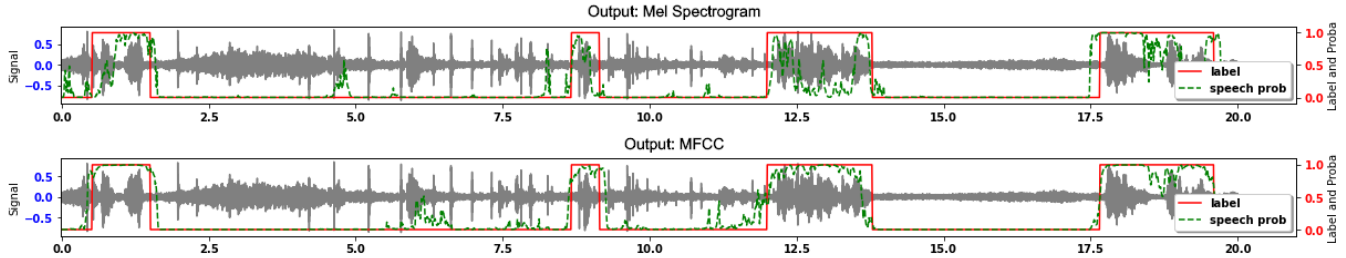


**Fig. 2.** Output plot of Mel spectrogram and MFCC. Example is from AVA-speech. The first two segments are speech with noise, the last two are speech with music.

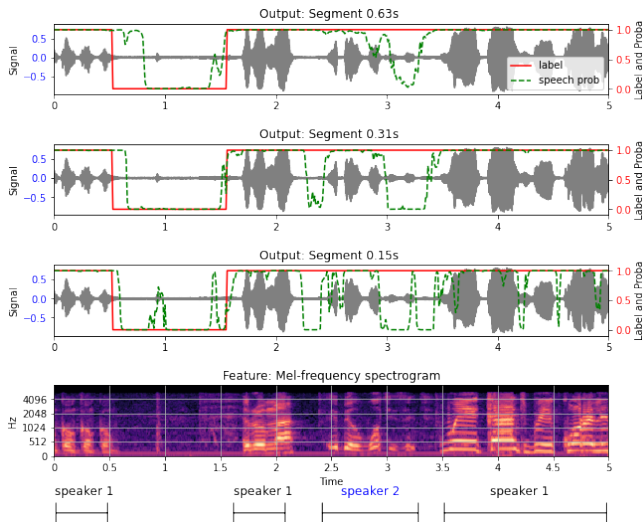


**Fig. 3.** Output plot of different segment lengths. Example is from AVA-speech.

### 3.5.3. Overlapping Predictions

Median and mean smoothing filters are generally used when generating frame level predictions [22, 16]. In Table 4, we show the results of these two filters using three different amounts of overlap: 12.5%, 50.0%, and 87.5%. We can see that model performance increases as the overlap increases. There is no significant difference between these two smoothing filters for the 87.5% overlap case.

**Table 4.** Model performance of *MarbleNet-3x2x64* using mean and median filters with 12.5%, 50%, and 87.5% overlap during inference on AVA-speech.

Smoothing filter	TPR for FPR=0.315				AUROC
	Clean	+Noise	+Music	All	All
Median 0.125	0.915	0.822	0.831	0.850	0.851
Median 0.500	0.933	0.829	0.837	0.860	0.861
Median 0.875	0.943	0.852	0.857	0.879	0.876
Mean 0.875	0.938	0.832	0.840	0.863	0.866

### 3.5.4. Noise Augmented Training

We compare *MarbleNet-3x2x64* trained with the basic augmentation described in Section 3.2, and without augmentation. Table 5 indicates that synthetic noise augmentation is helpful to improve the performance.

**Table 5.** *MarbleNet-3x2x64* trained with and without noise augmentation. Each result is averaged over 5 trials (95% Confidence Interval).

Augmentation	Clean	TPR for FPR=0.315		AUROC	
		+Noise	+Music	All	All
Basic	0.92±0.01	0.82±0.01	0.82±0.02	0.85±0.01	0.85±0.01
None	0.90±0.01	0.76±0.01	0.79±0.01	0.80±0.01	0.83±0.00

## 4. CONCLUSIONS

In this paper, we present *MarbleNet*, a computationally efficient, state-of-the-art deep Voice Activity Detection model. We evaluate *MarbleNet* on a diverse, multi-language, natural-sounding AVA-speech movie dataset. We demonstrate that *MarbleNet* is able to achieve state-of-the-art performance with 1/10th the parameters compared to the baseline model, which can make VAD more accessible under computationally constrained environments such as mobile and wearable devices. We conduct an extensive series of ablation studies to inspect the model’s behavior and serve as a guideline for future researchers and practitioners. Finally, by building the efficient yet lightweight *MarbleNet* with the open-source NeMo framework, we hope our work can facilitate wider adaptation of modern VAD technologies and democratization of AI.

**Acknowledgement** We would like to thank the NVIDIA AI Applications team for the help and valuable feedback.

## References

- [1] S. Chang, B. Li, G. Simko, T. N. Sainath, A. Tripathi, A. van den Oord, and O. Vinyals. Temporal modeling using dilated convolution and gating for voice-activity-detection. In *ICASSP*, 2018.
- [2] S. Chaudhuri, J. Roth, D. Ellis, A/ Gallagher, L. Kaver, R. Marvin, C. Pantofaru, N. Reale, L.G. Reid, K. Wilson, et al. Ava-speech: A densely labeled dataset of speech activity in movies. *arXiv:1808.00606*, 2018.

- [3] F. Chollet. Xception: Deep learning with depthwise separable convolutions. In *CVPR*, 2017.
- [4] T. DeVries and G.W. Taylor. Improved regularization of convolutional neural networks with cutout. *arXiv:1708.04552*, 2017.
- [5] S. Ding, Q. Wang, S. Chang, L. Wan, and I. Moreno. Personal VAD: Speaker-conditioned voice activity detection. *arXiv:1908.04284*, 2020.
- [6] F. Eyben, F. Weninger, S. Squartini, and B. Schuller. Real-life voice activity detection with LSTM recurrent neural networks and an application to hollywood movies. In *ICASSP*, 2013.
- [7] F. Font, G. Roma, and X. Serra. Freesound technical demo. In *ACM International Conference on Multimedia (MM'13)*, 2013.
- [8] G. Gelly and J. Gauvain. Optimization of RNN-based speech activity detection. *IEEE/ACM Transactions on Audio, Speech, and Language Processing*, 26(3):646–656, 2018.
- [9] K. He, X. Zhang, S. Ren, and J. Sun. Deep residual learning for image recognition. *arXiv:1512.03385*, 2015.
- [10] T. He, Z. Zhang, H. Zhang, Z. Zhang, J. Xie, and M. Li. Bag of tricks for image classification with convolutional neural networks. In *CVPR*, 2019.
- [11] R. Hebbar, K. Somandepalli, and S. Narayanan. Robust speech activity detection in movie audio: Data resources and experimental evaluation. In *ICASSP*, 2019.
- [12] L. Kaiser, A. Gomez, and F. Chollet. Depthwise separable convolutions for neural machine translation. *arXiv:1706.03059*, 2017.
- [13] D. P. Kingma and J. Ba. Adam: A method for stochastic optimization. *arXiv:1412.6980*, 2014.
- [14] S. Krivan, S. Beliaev, B. Ginsburg, J. Huang, O. Kuchaiev, V. Lavrukhin, R. Leary, J. Li, and Y. Zhang. QuartzNet: deep automatic speech recognition with 1D time-channel separable convolutions. *arXiv:1910.10261*, 2019.
- [15] O. Kuchaiev, J. Li, H. Nguyen, O. Hrinchuk, R. Leary, B. Ginsburg, S. Krivan, S. Beliaev, V. Lavrukhin, J. Cook, P. Castonguay, M. Popova, J. Huang, and J. Cohen. NeMo: a toolkit for building ai applications using neural modules. *arXiv:1909.09577*, 2019.
- [16] M. Lavechin, M. Gill, R. Bousbib, H. Bredin, and L. Garcia-Perera. End-to-end Domain-Adversarial Voice Activity Detection. *arXiv:1910.10655*, 2020.
- [17] J. Li, V. Lavrukhin, B. Ginsburg, R. Leary, O. Kuchaiev, J. Cohen, H. Nguyen, and R. Gadde. Jasper: An end-to-end convolutional neural acoustic model. *arXiv:1904.03288*, 2019.
- [18] Vitaliy Liptchinsky, Gabriel Synnaeve, and Ronan Collobert. Letter-based speech recognition with gated convnets. *arxiv:1712.09444*, 2017.
- [19] S. Majumdar and B. Ginsburg. MatchboxNet: 1d time-channel separable convolutional neural network architecture for speech commands recognition. *arXiv: 2004.08531*, 2020.
- [20] D. Park, W. Chan, Y. Zhang, C. Chiu, B. Zoph, E. Cubuk, and Q. Le. SpecAugment: A simple data augmentation method for automatic speech recognition. *arXiv:1904.08779*, 2019.
- [21] J. Ramirez, J. Górriz, and J. Segura. Voice activity detection. fundamentals and speech recognition system robustness. *Robust speech recognition and understanding*, 6(9):1–22, 2007.
- [22] A. Sehgal and N. Kehtarnavaz. A convolutional neural network smartphone app for real-time voice activity detection. *IEEE Access*, 6:9017–9026, 2018.
- [23] J. Sohn, N. Kim, and W. Sung. A statistical model-based voice activity detection. *IEEE signal processing letters*, 6(1):1–3, 1999.
- [24] I. Sutskever, J. Martens, G. Dahl, and G. Hinton. On the importance of initialization and momentum in deep learning. In *ICML*, 2013.
- [25] S. Thomas, S. Ganapathy, G. Saon, and H. Soltau. Analyzing convolutional neural networks for speech activity detection in mismatched acoustic conditions. In *ICASSP*, 2014.
- [26] P. Warden. Speech commands: A dataset for limited-vocabulary speech recognition. *arXiv:1804.03209*, 2018.
- [27] R. Zazo, T. Sainath, G. Simko, and C. Parada, editors. *Feature Learning with Raw-Waveform CLDNNs for Voice Activity Detection*, 2016.
- [28] R. Zazo-Candil, T. Sainath, G. Simko, and C. Parada. Feature learning with raw-waveform CLDNNs for voice activity detection. In *INTERSPEECH*, 2016.